scientific reports

Check for updates

OPEN

Atorvastatin calcium alleviates UVB-induced HaCat cell senescence and skin photoaging

Man Li[1], Yuchen Ge[1], Shirui Bai[1], Jing Xia[1], Guangming Wang[2], Yaxuan Zhang[1], Yuanyuan Zhang[2]✉, Xiaobo Wang[1]✉ & Min Zhou[1]✉

Excessive exposure to ultraviolet radiation B (UVB) has been shown to contribute to the aging of human skin cells. Previous research has demonstrated that atorvastatin calcium (Ato) can mitigate the aging effects caused by chemotherapy drugs. However, it remains unclear whether Ato can alleviate skin aging induced by ultraviolet radiation. In this study, through in vitro experiments with Hacat cells, we found that Ato can significantly reduce the UVB-induced increased expression of age-related protein p16 and age-related gene p21, and also reduce the up-regulation of inflammatory factors such as IL-1 and IL-6. Besides, it can reduce the expression of metallomatrix protein (MMP1 and MMP9), and inhibit cell senescence and inflammatory damage. Similarly, we found that Ato can enhance skin collagen fiber reduction and collagen volume decrease, repair skin photoaging and damage induced by UVB rays, and speed up the rate at which the wounded location heals in vivo using Balb/c mice. In the mechanism, Ato markedly decreased the expression of p-p38, p-p65, p-mTOR in vivo and in vitro, suggesting that it may act on Mitogen-activated protein kinase (MAPK), Nuclear factor κB (NF- κB) and Mammalian target of rapamycin (mTOR) signaling pathways to produce above marked effects. In conclusion, Ato obviously relieved UVB-induced photoaging and damage, thus providing evidence for its potential in mitigating skin aging caused by ultraviolet radiation.

Keywords Atorvastatin calcium, UVB, Cellular senescence, Skin photoaging

Ultraviolet B (UVB) is the intermediate frequency component of sunlight and plays a crucial role in synthesizing the basic compounds required for human physiological processes[1]. However, excessive exposure to ultraviolet radiation can lead to skin aging, with acute symptoms of skin burning, redness, swelling, blisters, and peeling of the outer layer of the skin. Over time, the skin will lose its elasticity, become rough, and manifest as sagging and wrinkling. In more severe cases, various clinical diseases may occur[2,3].

The process of skin damage caused by ultraviolet irradiation is multifaceted and intricate. A low dose of radiation allows the skin to withstand the effects of the radiation, an excessive amount damages the skin's protective barrier, obstructs the skin's ability to regulate itself, and causes senescent epidermal and dermal cells[4]. According to studies, excessive UVB exposure limits the ability of dermal cells that function as absorbers. Additionally, excessive UVB cannot be absorbed, causing Deoxyribonucleic acid (DNA) damage that triggers downstream signaling and the production of inflammatory cytokines. Moreover, prolonged exposure to UVB produces a lot of reactive oxygen species (ROS), which peroxides cell membranes. It has the capacity to cause acute inflammation, oxidative stress, apoptosis, and cell senescence[5,6]. On the one hand, the increase of ROS activates the IκBα kinase, which promotes the phosphorylation of IκBα and the release and activation of NF-κB. Activated NF-κB is transferred from the cytoplasm to the nucleus, binds to the corresponding DNA sequence, stimulates the expression of inflammatory factors, and thus promotes the occurrence of cell senescence[7]. On the other hand, the increase of ROS activates the p38-MAPK signaling pathway and participates in the processes of cell proliferation and differentiation and DNA damage reaction, which further leads to the occurrence of aging[8–10]. In addition, ultraviolet irradiation will continue to over-activate mTOR signal continuously, resulting in the improvement of cell metabolism, continuous growth and proliferation, directly or indirectly leading to the generation of photoaging[11,12].

Moreover, the dermis of the skin is mainly composed of collagen, reticular fiber, elastic fiber and matrix containing mucopolysaccharides, which play a key role in maintaining the normal toughness and elasticity of the skin[13]. After ultraviolet irradiation, the skin barrier effect is weakened, causing matrix metalloproteinases (MMPs) to be activated by the body, especially the expressions of MMP1 (collagenase) and MMP9 (gelatinase)

[1]School of Basic Medicine, Dali University, Dali 671000, Yunnan, China. [2]School of Clinical Medicine, Dali University, Dali 671000, Yunnan, China. ✉email: zhyy@dali.edu.cn; wxb4320062@163.com; may-zhoumin@163.com

to increase significantly. They degrade various extracellular matrix (ECM) components, decrease the elasticity of elastic fibers, and break collagen fibers, thus causing skin aging[14–16]. Currently, even anti-aging skincare products may contain harmful chemicals to the skin, such as benzoates and dimethylsiloxanes. These substances may pose potential hazards to the human body, not only affecting skin self-repair, but also affecting the endocrine system and increasing the risk of cancer[17,18]. Based on this, we need to explore drugs with significant effects and slight side effects to inhibit aging.

A well-known inhibitor of 3-hydroxy-3-methylglutaryl CoA (HMG-CoA) reductase is Ato. Studies have shown that Ato also has other pharmacological properties, such as antioxidant, anti-inflammatory, anti-aging and immune regulation. On the one hand, it can inhibit the enzyme source of ROS, leading to reduction of oxidative stress markers, thus playing an antioxidant role. On the other hand, it inhibits HMG CoA reductase, and further inhibits the synthesis of cholesterol and the production of isoprenoids, which leads to the decrease of valinization of small G proteins such as Rho. Then, it reduces NF-κB, enhances the expression of Kruppel-like fAtotor-2 (KLF2) and restrict NF-κB nuclear accumulation and DNA binding, which plays an anti-inflammatory and anti-aging role[19,20]. In the previous experiments, we proved that Ato has the effect of alleviating intestinal aging and reducing intestinal inflammation[21]. However, no research has shown that Ato also plays an anti-aging role in ultraviolet radiation.

In our study, we conducted a screening of frequently prescribed clinical therapeutic drugs and discovered that Ato, a commonly utilized anti-lipid medication, exhibits anti-inflammatory and anti-aging properties. However, the potential of Ato to inhibit UVB-induced aging and damage remains unverified. Therefore, we tried to carry out relevant anti-aging research on Hacat cells and Balb/c mouse back skin tissue. Through the detection of relevant aging indicators, we finally found that Ato effectively mitigates the detrimental effects of UVB-induced photoaging and damage.

Materials and methods

Reagents and antibodies

Atorvastatin calcium and dimethyl sulfoxide DMSO (cell culture grade) (Gat: D8371) were purchased from Solarboi (Beijing, China). L-glutamine (G0200) and penicillin mixture (100×) cell culture-specific (P1400) were from Solarbio (Beijing, China). Trypsin EDTA digestion solution (0.25%) (T1300) was from Solarboi (Beijing, China). MEM basic medium (PM150478) was purchased from Priscilla (Wuhan, China), Fetal Bovine Serum (C04001-050) was purchased from Viva Cell (Shanghai, China). MMP1 (10,371 2-AP, 1:1000) and MMP9 (10,375 2-AP, 1:1000) were from Proteintech (Wuhan, China). HRP conjugated Goat Anti-Rabbit IgG (H + L) (Cat#GB23303, 1:10,000) and HRP conjugated Goat Anti-Mouse IgG (H + L) (Cat#GB23301, 1:10,000) were purchased from Servicebio (Wuhan, China). Phospho-P38 MAPK (Thr180/Tyr182) Rabbit mAb (Cat#4511, 1:1500) Phospho-mTOR (Ser2448) (Cat#5536, 1:1000), and Phospho-NF-κB p65 (Ser536) (93H1) Rabbit mAb (Cat#3033, 1:1500) were purchased from Cell Signaling Technology (Danvers, MA). Antibody against GAPDH (Gat#GB15004, 1:2000) was from Servicebio (Wuhan, China). Anti-p16 (Cat#SR34-02, 1:1000) was purchased from Huabio (Hangzhou, China). Cell Counting Kit −8 Reagent (Gat#G4103) was purchased from Servicebio (Wuhan, China). Hematoxin-Eoain (HE) Stay Kit (Cat#G1120), MASSON's Trichrome Stay Kit (Cat#G1340), and Senescence-Associated-β-Galactosidase (SA-β-Gal) StayKit(Cat#G1580) were from Solarbio (Beijing, China).

Cell culture and treatment

We acquired human immortalized keratinocytes (Hacat) from Procell in Wuhan, China. They were planted in a mixed medium that contained 10% heat-inactivated fetal bovine serum, 1% L-glutamine, 1% streptomycin, and 88% MEM basic medium. The media was kept at 37 °C with 5% CO2 to allow for unrestricted growth and reproduction. For the purpose of the following investigation, the original Ato solution was dissolved in DMSO and diluted to a concentration of 10 mM. To mimic UVB irradiation, Xinzhi (Ningbo, China) supplied the Scientz 03-ii UV radiation system (312 nm, 60 W). According to the use of its instructions, we choose a wavelength of 312 nm (in the UVB wavelength range), and the irradiation distance is the distance between the light source and the 24-hole plate placed above the bottom of the box, about 15 cm. Because it is equipped with an ultraviolet energy programming system (Joules/ cm2), ultraviolet light exposure is continuously detected by a time integrator in it. When the energy absorption value reaches the set value, the irradiation will automatically stop. In our experiment, 40mj and 50mj energies were used to irradiate the cells, and the irradiation time was about 3–5s. Through the early exploration of the research group, it was found that using the following irradiation methods can cause more cells to age and relatively fewer cells to die. Hacat cells in good growth condition were inoculated into the cell culture plate. After overnight growth, we discarded the culture medium and immediately irradiated it with 40mj UVB. We then quickly added different concentrations of mixed culture medium and Ato solution, which was recorded as D1. Then, continued to grow overnight in a constant temperature incubator, we discarded the culture medium again and irradiated it again with 50mj UVB and added the culture medium and Ato solution to D2[16]. Finally, we collected samples corresponding to D3 and D5 days and tested relevant indicators.

Cell viability test

According to the above operation, 1000 Hacat cells were evenly seeded in 96 well plates, irradiated with UVB and added with different concentrations of Ato (0–3 μM) solution into the medium. The 96-well plate was kept in a constant temperature incubator for 96 h. Then, 5 μL CCK-8 reagent and 95 μL medium mixed to form 100 μL of a new solution, and added to 96 well plates to continue to grow at 37 ℃ in 5% CO_2. After 1 h, the absorbance of each well at 450 nm was measured by a microplate reader. The mean value ± SD is used to express the results.

Animal experiment

Animal experiments were performed using routinely cultured 8-week-old healthy male Balb/c mice from Chushang Biotechnology (Yunnan, China). We declare that the animal experiment plan carried out has been accepted by the Experimental Animal Organizing Committee of Dali University (No.2022-p2-21) on February 10, 2022. All methods were carried out in accordance with relevant guidelines and regulations, and are reported in accordance with ARRIVE guidelines. The minimum number of samples was calculated according to the resource equation "E = N-K = Kn-K = K (n-1)". Where N is the total number of experimental units; n is the sample size of each group; K is the number of treatment groups, which is 3 groups in this experiment; E is the difference, which has a minimum value of 10 and a maximum value of 20. According to the equation, N is calculated to be 13. So, the total number was 15 after a slight correction due to the grouping of three groups. During the experiment, in order to prevent accidental death of mice and ensure that the experiment could be completed at one time, we added one mouse per group to the planned number as appropriate to avoid the use of more mice for the failure of the experiment. Initially, they were kept in an environment with a typical day-night cycle, temperature of 23 ± 1 °C, and humidity levels of 40%–60%. After a week of acclimation, the mice were given unrestricted access to food and water. The mice were put to sleep using a small animal anesthesia machine (ABM-100, Shanghai, China), and the anesthetic drug was Isoflurane (Gat: Isoflurane) purchased from Yuyan Scientific Instrument Co., LTD. (Shanghai, China), and day 0 was marked by the removal of the mice's back hair. Following the first day of back hair removal, 18 mice were randomly assigned to 3 groups, each of which received 6 treatments: PBS treatment just as the blank control group, UVB irradiation + PBS treatment, and Ato treatment group (UVB irradiation + Ato therapy). Irradiation was performed using the above apparatus, and the irradiation distance was the distance between the light source and the skin on the back of the mouse above the bottom of the chamber, the energy was chosen to be 75 mj, and the irradiation time was about 7 s. For clinical use, 10 mg of Ato is recommended. It is translated to the corresponding dose for humans and animals and administered using a 0.1 μM diluent. For seven days in a row, PBS or Ato was administered equally to each mouse's back. Ultimately, the mice were put down on the eighth day by cervical dislocation under deep anesthesia using the above method, and the skin tissue from their backs was removed for additional research.

Senescence-associated-β-galactosidase (SA-β-Gal) staining

The cells were placed on 24-well plates, exposed to UVB radiation twice using the same technique, and then given the Ato treatment. After five days of culture, the cells were stained. After removing the medium, the cells underwent one PBS wash, the fixed solution was applied, and they were left to fix for fifteen minutes at room temperature. The cells were treated with PBS three times for five minutes each, and then they were incubated with the staining solution for a whole night at 37 °C. Ultimately, an optical microscope (Olympus IX71, Shanghai, China) was used to see and take pictures of the cells. Senescent Hacat cells can be stained blue-green by senescent cell counting, which indicates the efficacy of the medication. The mean ± SD for three replicates is used to express the results.

The frozen slice of mouse back skin was 5 μm thick and stained with SA-β-Gal. Added the fixing solution and place it on the surface of the sample, fixed it at room temperature for 15 min, and then washed it with PBS 3 times for 5 min each time. Blotted out PBS with filter paper, added dye solution to completely cover the sample, and placed in an incubator at 37℃ overnight. Finally, the PBS washing dye was observed and photographed under a microscope (Olympus IX71, Shanghai, China).

Histological analysis and measurement of dorsal thickness

Freeze slice the skin tissue on the back of mice with a thickness of 5 μm. Then, placed the slices at room temperature for rewarming, and performed histological staining on the slices according to the instructions for H&E staining and Masson staining. Sealed and stored the stained slices with neutral resin. Finally, placed the slices under an Olympus (IX71) microscope, took photos and measured the thickness of the epidermis. Inflammatory factors and collagen volume were statistically analyzed using ImageJ software.

Western blot

The total proteins in cells or mouse skin tissues were extracted with cryolysis buffer and 2.5 × SDS loading buffer and quantified (Bio-Rad). The extracted samples were added to 8% and 12% SDS-PAGE gels for electrophoretic separation, and the separated proteins were transferred to PVDF membrane (milibo, Germany) and sealed with 5% skimmed milk at room temperature for 1 h. Then, the specific primary antibody was added to the 5% BSA diluent According to the diluted concentration in the instructions, and the diluted antibody was used to cover the protein band, and incubated overnight at 4 ℃. Next, it was washed the primary antibody with TPST solution 3 times, each time for 5 min, and the relatively specific secondary antibody was added to 5% skimmed milk at a concentration of 1:10,000. After incubation at room temperature for 1 h, it was washed three times with TPST solution for 5 min each time. Finally, ECL plus Western blot Kit (bio rad, Hercules, CA) and fusion solo imaging system (Germany) were used for protein band development. The gray value of the strip is quantified by ImageJ analysis software. The experiment was repeated three times.

Real-time quantitative polymerase chain reaction detecting

Trizol reagent (Takara, Shiga, Japan) was used to extract total RNA from cells or mice skin tissues, and cDNA Synthesis Super Mix (Cat#G3337-50, Servicebio, Wuhan, China) was used for reverse transcription. Next, quantitative real-time polymerase chain reaction (qRT-PCR) was performed using SYBR Green qPCR Master Mix (Cat#G3320-15, Servicebio, Wuhan, China). Using the 18SRNA sequence as a control, the relative amount of cDNA was calculated by comparing the target CT value, and the corresponding mRNA expression was ascertained. There were three iterations of the experiment. The following are the PCR amplification primers:

Primer Name	Primer Sequence
18S-F	TTGACGGAAGGGCACCACCAG
18S-R	GCACCACCACCCACGGAATCG
hp21-F	TGTCCGTCAGAACCCATGC
hp21-R	AAAGTCGAAGTTCCATCGCTC
hIL-1β -F	ACAGGCTGCTCTGGGATTCT
hIL-1β-R	ACAGGCTGCTCTGGGATTCT
hIL-6-F	GTGTGAAAGCAGCAAAGAG
hIL-6-R	CTCCAAAAGACCAGTGATG
mIL-1-F	TGGACCTTCCAGGATGAGGACA
mIL-1-R	TGGACCTTCCAGGATGAGGACA
mIL-6-F	ACTCACCTCTTCAGAACGAATTG
mIL-6-R	CCATCTTTGGAAGGTTCAGGTTG

Statistical analysis

Student's t-test was used to examine the differences between different groups, and Bonferroni post-hoc one-way analysis of variance was used to examine the differences between groups. $p < 0.05$ is defined as statistically significant, $p < 0.01$ is remarkably significant, and $p < 0.001$ is highly significant. The results are expressed as the mean ± SD of at least three replicates.

Results

Atorvastatin calcium inhibits UVB-induced cell senescence in Hacat

We used the UVB irradiation method described above to explore the anti-aging effect of Atorvastatin calcium (Fig. 1a) on Hacat cells. In Fig. 1b-c, we used SA-β-Gal stained Hacat cells and the results showed that only the UVB-irradiation group had a significant increase in the proportion of blue-green aging cells. While using Ato can greatly reduce the proportion of aging cells. With the concentration of Ato increased, the blue-green cells also decreased, but the cell morphology began to change with the concentration increased, and the concentration

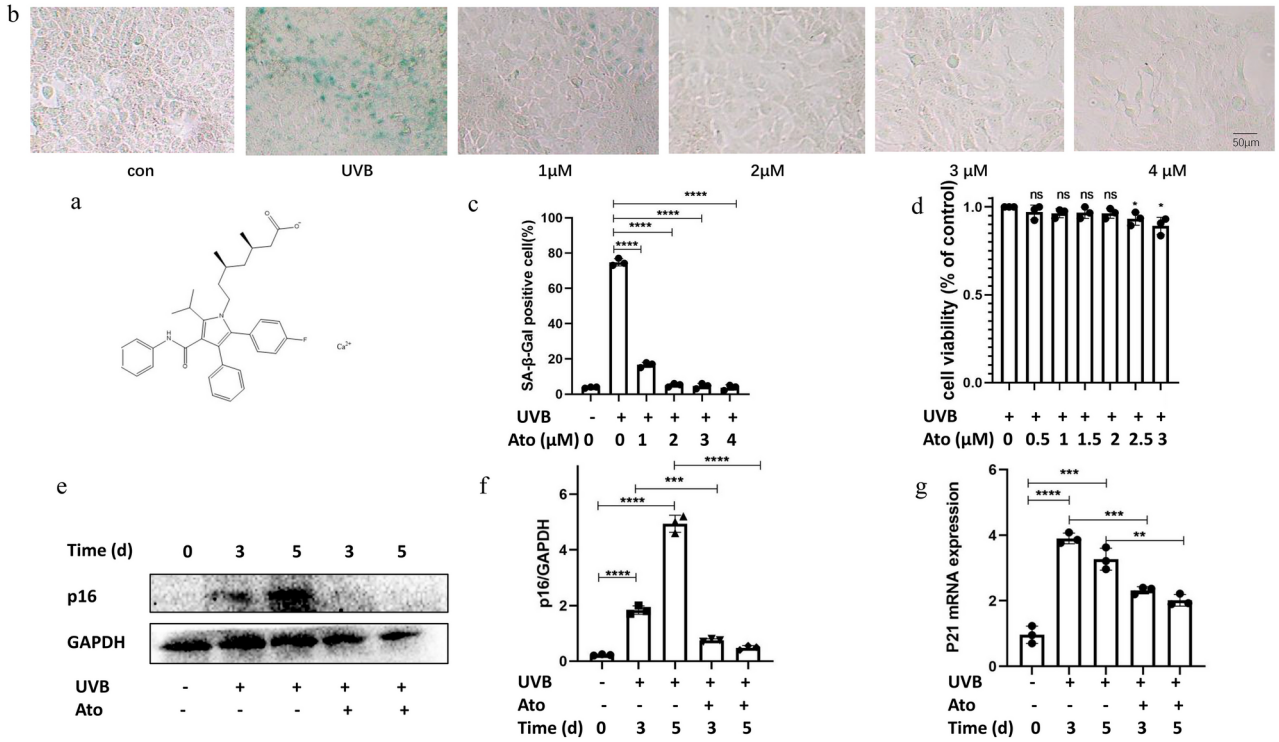

Fig. 1. (**a**) Calcium atorvastatin's chemical composition. (**b**) Plots stained with SA-β-Gal and varying amounts of Ato. (**c**) The proportion of cells positive for SA-β-Gal, as indicated in (**b**). (**d**) Viability of Hacat cells following the application of Ato (0–3 μM). (**e**) GAPDH and p16 Western Blot. (**f**) The quantification of p16 protein levels using pictures from three separate tests, as indicated in (**e**). (**g**) P21 mRNA level relative fold changes as assessed by qRT-PCR. In comparison to the vehicle control, *$p < 0.05$, **$p < 0.01$, ***$p < 0.001$, and ****$p < 0.0001$.

reached 3 μM, and cell morphology became larger and rounder. CCK8 cell viability test (Fig. 1d) also showed that a low concentration of Ato had no effect on cell viability, but when the concentration of Ato reached 2.5 μM, the cell viability decreased significantly. To further analyze the anti-aging efficacy of Ato, we performed Western blotting and RT-qPCR. Previous studies have shown that P16 is a key effector during cellular senescence. P16 expression increase will promote age-related marker gene p21 expression, resulting in cell senescence (DOI: https://doi.org/10.1101/2023.12.05.569858). As shown in Fig. 1e-f, UVB-irradiation significantly increased the expression of p16 protein, but the expression was down-regulated after treatment with Ato. Besides, RT-qPCR results showed that the mRNA expression of the p21 gene also showed a downward trend in the Ato treatment group (Fig. 1g). Ato can reduce the expression of aging-related proteins p16 and aging-related genes p21 in aging cells. These results suggested that Ato can effectively alleviate UVB-induced cell aging.

Atorvastatin calcium inhibits UVB-induced inflammation in Hacat

In previous experiments, we have proved that Ato can inhibit UVB-induced cell senescence. How does it inhibit senescence? We screened the aging related signaling pathways. The WB results of Fig. 2a-d showed that the expression of p-mTOR, p-p38 and p-p65 increased only in the UVB irradiation group. While treatment with Ato, the expression of these proteins decreased significantly. These results indicated that Ato played an important role in the anti-aging effect of Hacat cells induced by UVB, they might be related to mTOR, MAPK and NF-κB signal pathways. The process of aging is often accompanied by inflammation[20]. We detected the mRNA expression of inflammatory factors IL-1 and IL-6 (Fig. 2e-f) by RT-qPCR, and found that Ato can effectively reduce the inflammatory factors produced after UVB irradiation. They indicated that it can inhibit the inflammation of Hacat cells induced by UVB. Studies have shown that the increase of inflammatory factors can activate matrix metalloproteinases in the body and degrade a variety of extracellular matrix (ECM) components. Among them, MMP1 and MMP9 are common matrix metalloproteinases, and their increased expression can degrade ECMs components, reduce the elasticity of elastic fibers, and damage collagen fibers, which can lead to skin aging[15]. Therefore, MMPs reflected the degree of inflammation damage caused by photoaging to a certain extent. As shown in Fig. 2g-i, the expressions of MMP1 and MMP9 were up-regulated after UVB irradiation, but both showed a downward trend after Ato was used. In conclusion, Ato not only inhibited the aging of Hacat cells induced by UVB, but also inhibited the inflammatory reaction accompanying the aging process, reduced the expression of matrix metalloproteinases caused by UVB irradiation, and reduced the damage of photoaging.

Atorvastatin calcium inhibits UVB-induced skin photoaging in Balb/c mice

We have proved the anti-aging effect of Ato through cell experiments, and we verified it in mice. We selected the back skin tissue of Balb/c mice for UVB irradiation to form a model of skin photoaging and damage in Fig. 3a. As shown in Fig. 3b, UVB irradiation caused obvious redness and swelling, flaky erythema, and in severe cases, spotty bleeding, crusting and other injuries on the back skin of mice. These symptoms were most obvious on

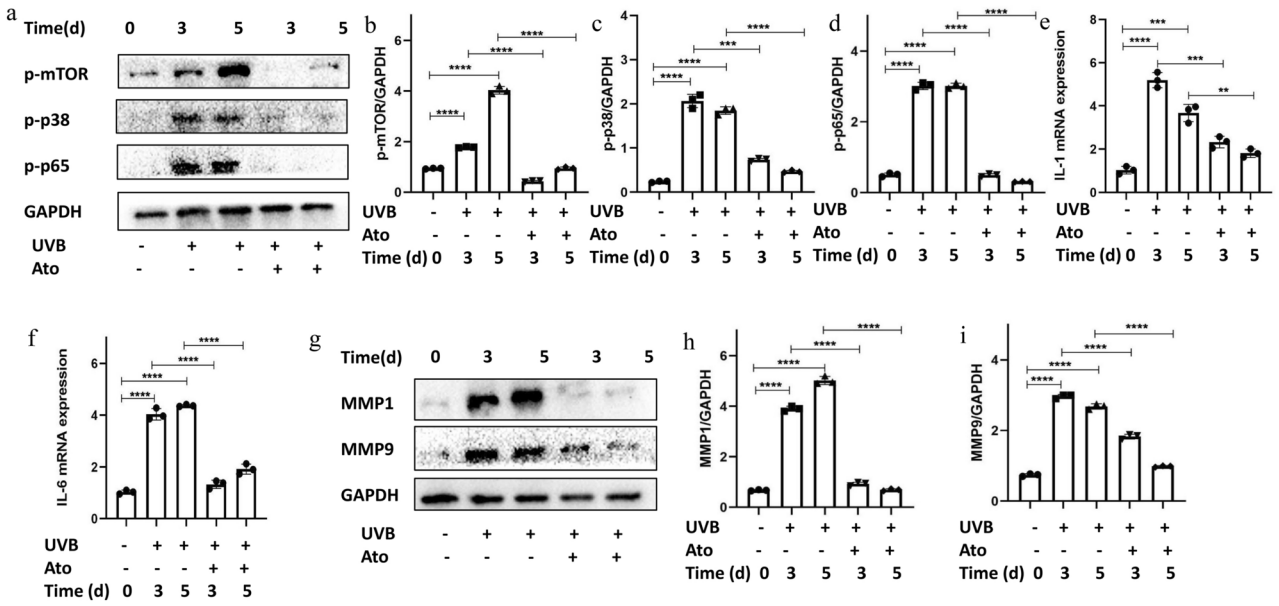

Fig. 2. Atorvastatin calcium inhibits UVB-induced inflammation. (**a**) Western Blot analysis of GAPDH, p-mTOR, p-p38, and p-p65. (**b**) Quantification of p-mTOR protein levels using pictures from (**a**). (**c**) Quantification of p-p38 protein levels using pictures from (**a**). (**d**) Quantification of p-p65 protein levels using pictures from (**a**). (**e**) Comparative fold-changes in the IL-1 mRNA level as assessed by qRT-PCR. (**f**) Comparative fold-changes in the IL-6 mRNA level as assessed by qRT-PCR. (**g**) MMP1, MMP9, and GAPDH Western Blot. (**h**) Quantification of MMP1 protein levels using pictures from (**g**). (**i**) Quantification of MMP9 protein levels using pictures from (**g**). In comparison to the vehicle control, $^{*}p < 0.05$, $^{**}p < 0.01$, $^{***}p < 0.001$, and $^{****}p < 0.0001$.

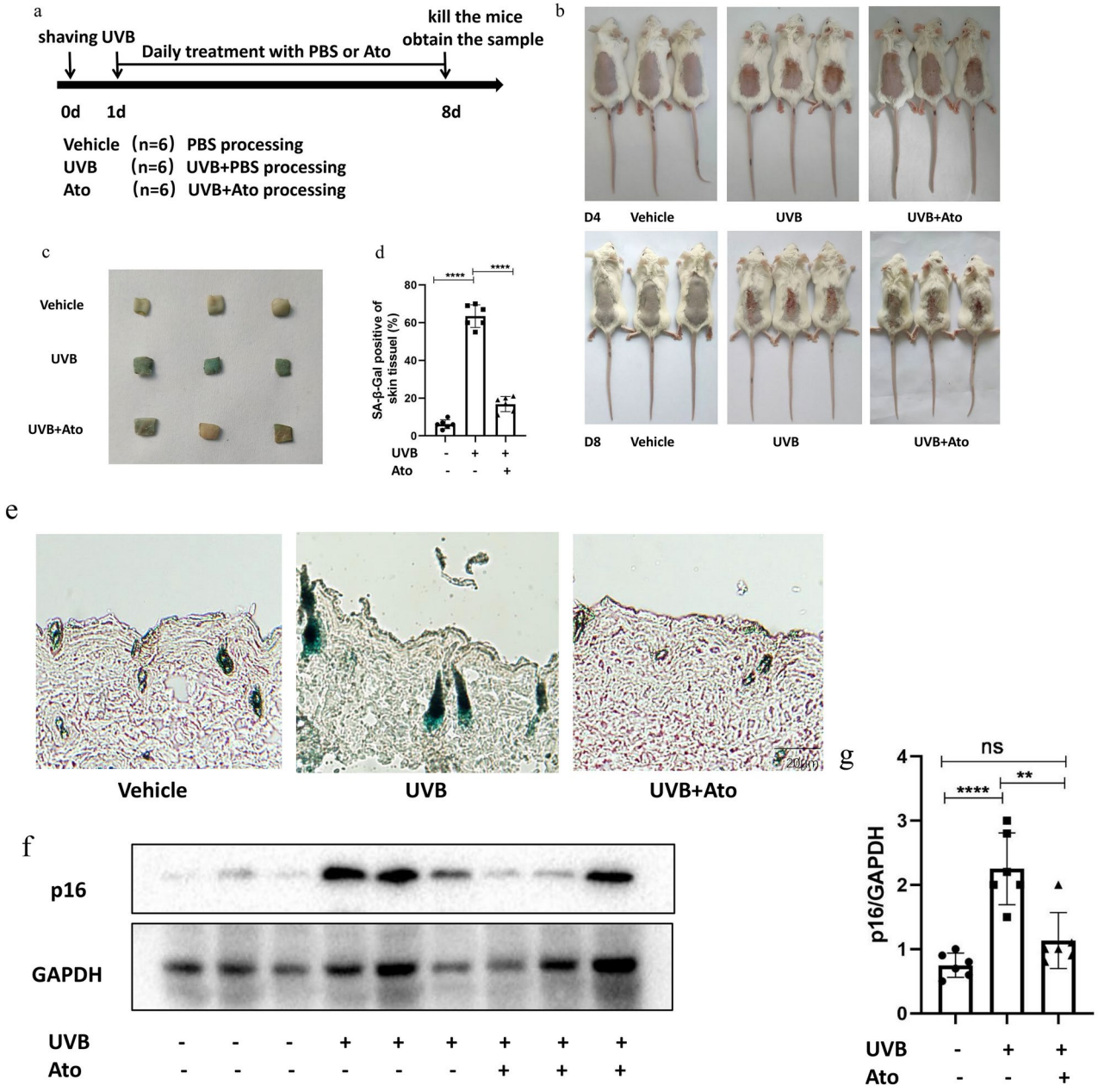

Fig. 3. Atorvastatin calcium inhibits UVB induced skin photoaging in Balb/c mice. (**a**) Schematic diagram for animal experiment modeling and therapy. (**b**) The fourth and eighth days show the schematic diagram of the erythema and scar on the back skin of the Balb/c mice. (**c**) Skin tissue blocks on the back of Balb/c mice stained with SA-β-Gal. (**d**) The skin tissue of (**c**) has a positive rate of SA-β-Gal. (**e**) SA-β-Gal staining of frozen mouse back skin slices (Balb/c strain). (**f**) Western Blot analysis of GAPDH and p16. (**g**) Quantification of p16 protein levels using the pictures from (**f**). In comparison to the vehicle control, $^{*}p < 0.05$, $^{**}p < 0.01$, $^{***}p < 0.001$, and $^{****}p < 0.0001$.

the fourth day. When the mice were treated on the 8th day, the skin on the back was thickened with naked eyes, crusted and hardened, and there was obvious bleeding after removing the crusts. The use of Ato treatment made the skin damage of mice lighter, the erythema phenomenon was significantly reduced, the damaged area was also relatively reduced, and there was no obvious crusting and hardening of the skin. Moreover, the SA-β-Gal staining of the skin tissue or frozen section in the UVB irradiation group show obvious blue staining, while the blue staining in Ato treatment group was significantly reduced, and with significant statistical significance (Fig. 3c-e). Besides, the WB results of Fig. 3f showed that use of treatment with Ato, the expression of p16 protein was significantly decreased compared with the UVB irradiation group, this is consistent with the statistical results in Fig. 3g, and p16 protein was a sensitive indicator of cell aging. The results of SA-β-Gal staining and p16 protein detection showed that Ato effectively alleviated mouse skin aging. In conclusion, Ato can effectively inhibit UVB-induced skin photoaging in Balb/c mice.

Atorvastatin calcium attenuates UVB-induced skin inflammation in mice

In addition to reducing UVB-induced skin photoaging in mice, Ato also significantly reduces inflammatory damage. The HE staining results of frozen sections of mouse back skin tissue in Fig. 4a demonstrated that UVB irradiation significantly thickened the mouse skin's epidermis and increased the infiltration of inflammatory factors (Fig. 4b-c). However, the degree of skin damage was reduced and the situation that led to the above was significantly improved by Ato treatment. In addition, RT-qPCR results (Fig. 4d-e) showed that UVB irradiation significantly increased the expression of inflammatory factors IL-1 and IL-6 in the skin of mice, and Ato could effectively reduce the expression of these inflammatory factors and reduce the skin damage caused by UVB. Furthermore, WB results showed that after UVB irradiation, the expression of p-mTOR, p-p38 and p-p65 in Balb/c mouse skin was significantly increased (Fig. 4f-i). However, the expression in the Ato treatment group did not increase, indicating that Ato may act on mTOR, MAPK, NF- κB signaling pathway plays an anti-inflammatory role. In Fig. 4j, Masson staining of frozen sections showed that UVB irradiation led to the decrease of collagen fibers and collagen volume (Fig. 4k), while Ato could increase the number of collagen fibers and improve the speed of injury repair. The detection results of MMPs by WB showed that UVB irradiation increased the expression of MMP1 and MMP9, which would lead to the degradation of extracellular matrix components and further aggravate the skin damage, but Ato effectively improved this process and repaired the skin damage (Fig. 4l-n). In a word, Ato may through mTOR, MAPK and NF-κB signaling pathway reduce the skin inflammatory injury induced by UVB in mice, reduce the expression of matrix metalloproteinases, and accelerate the repair speed of the injured site.

Discussion

Ato can inhibit HMG-CoA reductase and is used in clinical practice to reduce cholesterol levels in the blood. At present, research has found that it has anti-inflammatory, anti-aging and other effects[22]. In this article, we demonstrate that Ato not only effectively inhibits UVB-induced senescence and inflammation of Hacat cells, but also significantly reduces skin photoaging and inflammatory damage in Balb/c mice induced by UVB. Previous studies showed that the HMG CoA inhibitors can inhibit cell proliferation, induction of cell cycle G1 stagnation and apoptosis, and by reducing the HMG CoA of enzyme activity and inhibition of ovarian cancer cells MAPK and mTOR pathway caused by stress. In addition, HMG-CoA inhibitors can treat oxidative stress and tissue damage diseases by targeting intracellular ROS and NF-κB[23,24]. As a classic HMG-CoA inhibitor, Ato may reduce UVB-induced inflammatory damage and aging by inhibiting the enzyme activity of HMG-CoA and targeting MAPK, NF-κB and mTOR signaling pathways. The preliminary exploration in our experiment. Through WB experiments, we found that Ato treatment group reduced UVB-induced p-p65 and p-p38 protein levels in Hacat cells, indicating that the anti-inflammatory and anti-aging effects of Ato may be related to MAPK and NF-κB signaling pathways. In addition, we also detected the expression of p-mTOR protein and found that the anti-aging effect of Ato may also be related to the mTOR signal. It is widely believed that the mTOR signaling pathway plays a crucial role in mammalian aging[25]. Excessive exposure to UVB causes DNA damage, activates the mTOR signaling pathway, increases the level of cell metabolism, and continues growth and proliferation. This causes the cells damaged by DNA to arrest in circulation and transform into senescent cells, which leads to the occurrence of skin photoaging[26]. Several lines of evidence suggest that during mTOR inhibition, mRNA translation is generally reduced and slows aging by reducing proteotoxicity and the accumulation of oxidative stress[27–29]. In our experiment, after application of Ato, the expression of p-mTOR detected by WB showed a significant downward trend. It suggesting that Ato may act on factors in the mTOR signaling pathway to alleviate DNA damage and inhibit photoaging by reducing oxidative stress in cells. Although we preliminarily screened in this experiment that the anti-aging and anti-inflammatory effects of Ato may be related to the mTOR, MAPK and NF-κB pathways, the relevant pathway blocking experiments have not been carried out to confirm this correlation, which is also the main content of further research.

The dermis is rich in extracellular matrix (ECM), which is mainly responsible for maintaining skin structure and elasticity[30]. Matrix metalloproteinase (MMP) is responsible for the degradation of ECM. When MMP expression is increased, the ECM is decomposed, the skin structure is damaged, and the elasticity is decreased, showing the trend of aging[31]. Among UV-induced MMP genes, MMP1, MMP3 and MMP9 are generally considered to be the major mediators of photoaging. MMP-1 can degrade collagen fiber bundles, and MMP-9 can further degrade collagen cleaved by MMP-1, thus degrading collagen, causing skin to lose elasticity and become wrinkled and wrinkle[32,33]. In our experiment, we detected the protein expression of MMPs by WB assay and found that Ato could effectively reduce the UVB-induced increased expression of MMP1 and MMP9. In addition, through the statistical analysis of the collagen volume in the Masson staining section diagram, it can also be seen that Ato significantly inhibits the collagen interpretation, thereby protecting the skin and resisting aging.

UVB irradiation causes an increase in ROS levels in the skin, and the accumulation of ROS during aging can lead to lipid peroxidation and membrane damage, etc., causing skin barrier disruption, which leads to cell death[6,34]. After acute barrier disruption, cholesterol synthesis in the epidermis is rapidly and significantly increased, which is associated with increased HMG-CoA reductase activity, protein, and mRNA levels[34–36]. We applied Ato to the skin surface of mice and speculated that it could inhibit the activity of HMG-CoA reductase, inhibit the increase in epidermal cholesterol synthesis, and alleviate the skin barrier dysfunction caused by UVB damage. This enables skin self-regulatory mechanisms to resist UVB radiation and play an anti-aging role, inhibiting UVB-induced cellular senescence and inflammatory damage. Therefore, we hypothesize that anti-skin photoaging agents can target inhibition of HMG-CoA reductase, which is also a direction that can be further explored in the future.

Our study is the first to demonstrate that Ato can inhibit photoaging, which provides some evidence for subsequent studies of Ato anti-aging. Ato can be used to reduce UV-induced skin aging and damage in vitro

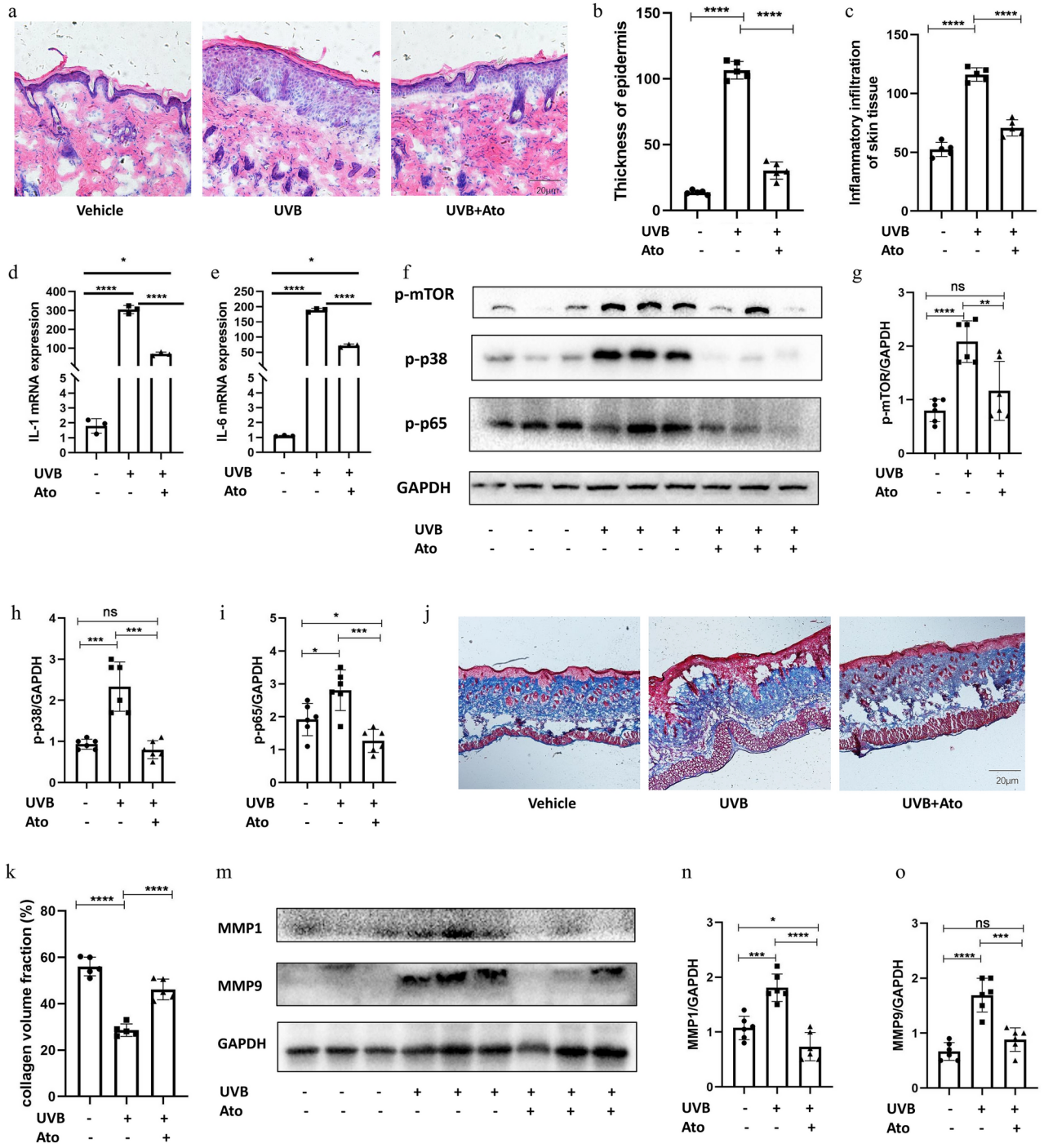

Fig. 4. Atorvastatin calcium attenuates UVB induced skin inflammation in mice. (**a**) Skin tissue slices from Balb/c mice stained with H&E. (**b**) A statistical chart showing the skin's epidermal thickness in Balb/c mice (**a**). (**c**) Statistical diagram showing the infiltration of inflammation in the skin of Balb/c mice (**a**). (**d**) Relative fold-changes measured by qRT-PCR in the IL-1 mRNA level. (**e**) Comparative fold-changes in the IL-6 mRNA level as assessed by qRT-PCR. (f) GAPDH, p-mTOR, p-p38, and p-p65 Western blot. (**g**) Quantification of p-mTOR protein levels using pictures from three separate studies, as indicated in (**f**). (**h**) P-p38 protein levels were measured using the images from three separate studies, which are displayed in (**f**). (**i**) p-p65 protein levels were measured using the three separate experiments' pictures, which are displayed in (**f**). (**j**) Masson staining of skin tissue slices from Balb/c mice. (**k**) A statistical chart showing the skin's collagen volume in Balb/c mice (**j**). (**l**) Western Blot analysis of GAPDH, MMP1, and MMP9. (**m**) MMP1 protein levels were measured using the pictures from three different tests, which are displayed in (**l**). (**n**) Quantification of MMP9 protein levels using pictures from three separate studies, as displayed in (**l**) In comparison to the vehicle control, $^{*}p < 0.05$, $^{**}p < 0.01$, $^{***}p < 0.001$, and $^{****}p < 0.0001$.

and in vivo. Therefore, attempts can be made to develop protective agents based on Ato to protect the skin barrier function, promote the metabolism of epidermal lipids, and prevent skin aging. The use of anti-aging drugs to resist skin aging may be a new anti-aging strategy, which can inhibit skin aging, but also further delay the occurrence of systemic aging and age-related diseases, providing a new strategy for clinical diagnosis and treatment.

Data availability

The corresponding author can provide the datasets created and/or analyzed during the current work upon reasonable request.

Received: 22 February 2024; Accepted: 27 November 2024
Published online: 03 December 2024

References

1. Ezekwe, N., Maghfour, J. & Kohli, I. Visible Light and the Skin. *Photochemistry and photobiology.* **98**, 1264–1269. https://doi.org/10.1111/php.13634 (2022).
2. Guan, L. L., Lim, H. W. & Mohammad, T. F. Sunscreens and Photoaging: A Review of Current Literature. *American journal of clinical dermatology.* **22**, 819–828. https://doi.org/10.1007/s40257-021-00632-5 (2021).
3. Passeron, T. et al. Photoprotection according to skin phototype and dermatoses: practical recommendations from an expert panel. *Journal of the European Academy of Dermatology and Venereology: JEADV.* **35**, 1460–1469. https://doi.org/10.1111/jdv.17242 (2021).
4. Katayama, S. et al. Lacticaseibacillus paracasei K71 Alleviates UVB-Induced Skin Barrier Dysfunction by Attenuating Inflammation via Increased IL-10 Production in Mice. *Molecular nutrition & food research.* **67**, e2200212. https://doi.org/10.1002/mnfr.202200212 (2023).
5. Kawashima, S. et al. Protective effect of pre- and post-vitamin C treatments on UVB-irradiation-induced skin damage. *Scientific reports.* **8**, 16199. https://doi.org/10.1038/s41598-018-34530-4 (2018).
6. Zhang, D. et al. Echinacoside Alleviates UVB Irradiation-Mediated Skin Damage via Inhibition of Oxidative Stress, DNA Damage, and Apoptosis. *Oxidative medicine and cellular longevity.* **2017**, 6851464. https://doi.org/10.1155/2017/6851464 (2017).
7. Salminen, A., Kauppinen, A. & Kaarniranta, K. AMPK activation inhibits the functions of myeloid-derived suppressor cells (MDSC): impact on cancer and aging. *Journal of molecular medicine (Berlin, Germany).* **97**, 1049–1064. https://doi.org/10.1007/s00109-019-01795-9 (2019).
8. Zhou, M., Liu, Z. L., Liu, J. Y. & Wang, X. B. Tedizolid phosphate alleviates DSS-induced ulcerative colitis by inhibiting senescence of cell and colon tissue through activating AMPK signaling pathway. *International immunopharmacology.* **135**, 112286. https://doi.org/10.1016/j.intimp.2024.112286 (2024).
9. Jia, H. et al. Anti-inflammation and anti-aging mechanisms of mercaptopurine in vivo and in vitro. *Biochemical and biophysical research communications.* **638**, 103–111. https://doi.org/10.1016/j.bbrc.2022.11.035 (2023).
10. Ge, Y., Zhou, M., Chen, C., Wu, X. & Wang, X. Role of AMPK mediated pathways in autophagy and aging. *Biochimie.* **195**, 100–113. https://doi.org/10.1016/j.biochi.2021.11.008 (2022).
11. An, S. et al. Inhibition of 3-phosphoinositide-dependent protein kinase 1 (PDK1) can revert cellular senescence in human dermal fibroblasts. *Proceedings of the National Academy of Sciences of the United States of America* **117**, 31535–31546. https://doi.org/10.1073/pnas.1920338117 (2020).
12. Carr, T. D., DiGiovanni, J., Lynch, C. J. & Shantz, L. M. Inhibition of mTOR suppresses UVB-induced keratinocyte proliferation and survival. *Cancer prevention research (Philadelphia, Pa.)* **5**, 1394–1404, https://doi.org/10.1158/1940-6207.Capr-12-0272-t (2012).
13. Solano, F. Metabolism and Functions of Amino Acids in the Skin. *Advances in experimental medicine and biology.* **1265**, 187–199. https://doi.org/10.1007/978-3-030-45328-2_11 (2020).
14. Kim, D. J., Iwasaki, A., Chien, A. L. & Kang, S. UVB-mediated DNA damage induces matrix metalloproteinases to promote photoaging in an AhR- and SP1-dependent manner. *JCI insight.* **7**, https://doi.org/10.1172/jci.insight.156344 (2022).
15. Jia, H. J., Ge, Y., Xia, J., Shi, Y. L. & Wang, X. B. Belinostat (PXD101) resists UVB irradiation-induced cellular senescence and skin photoaging. *Biochemical and biophysical research communications.* **627**, 122–129. https://doi.org/10.1016/j.bbrc.2022.08.038 (2022).
16. Ge, Y. et al. Doxercalciferol alleviates UVB-induced HaCaT cell senescence and skin photoaging. *International immunopharmacology.* **127**, 111357. https://doi.org/10.1016/j.intimp.2023.111357 (2024).
17. Waters, A. J., Sandhu, D. R., Lowe, G. & Ferguson, J. Photocontact allergy to PABA in sunscreens: the need for continued vigilance. *Contact dermatitis.* **60**, 172–173. https://doi.org/10.1111/j.1600-0536.2008.01448.x (2009).
18. Funk, J. O., Dromgoole, S. H. & Maibach, H. I. Sunscreen intolerance. Contact sensitization, photocontact sensitization, and irritancy of sunscreen agents. *Dermatologic clinics.* **13**, 473–481 (1995).
19. Xu, X. et al. Anti-inflammatory and immunomodulatory mechanisms of atorvastatin in a murine model of traumatic brain injury. *Journal of neuroinflammation.* **14**, 167. https://doi.org/10.1186/s12974-017-0934-2 (2017).
20. Jain, M. K. & Ridker, P. M. Anti-inflammatory effects of statins: clinical evidence and basic mechanisms. *Nature reviews. Drug discovery.* **4**, 977–987. https://doi.org/10.1038/nrd1901 (2005).
21. Xia, J. et al. Atorvastatin calcium alleviates 5-fluorouracil-induced intestinal damage by inhibiting cellular senescence and significantly enhances its antitumor efficacy. *International immunopharmacology.* **121**, 110465. https://doi.org/10.1016/j.intimp.2023.110465 (2023).
22. Oliveira-Junior, S. A., Carvalho, M. R., Mendonça, M. L. M. & Martinez, P. F. Anti-Inflammatory Effects of Atorvastatin Therapy in Metabolic Syndrome. *Arquivos brasileiros de cardiologia.* **117**, 748–749. https://doi.org/10.36660/abc.20210720 (2021).
23. Nabi, R. et al. Modulatory role of HMG-CoA reductase inhibitors and ezetimibe on LDL-AGEs-induced ROS generation and RAGE-associated signalling in HEK-293 Cells. *Life sciences.* **235**, 116823. https://doi.org/10.1016/j.lfs.2019.116823 (2019).
24. Stine, J. E. et al. The HMG-CoA reductase inhibitor, simvastatin, exhibits anti-metastatic and anti-tumorigenic effects in ovarian cancer. *Oncotarget.* **7**, 946–960. https://doi.org/10.18632/oncotarget.5834 (2016).
25. Chen, Z., Li, C., Huang, H., Shi, Y. L. & Wang, X. Research Progress of Aging-related MicroRNAs. *Current stem cell research & therapy.* **19**, 334–350. https://doi.org/10.2174/1574888x18666230308111043 (2024).
26. Chen, Q. et al. Metformin Attenuates UVA-Induced Skin Photoaging by Suppressing Mitophagy and the PI3K/AKT/mTOR Pathway. *International journal of molecular sciences.* **23**, https://doi.org/10.3390/ijms23136960 (2022).
27. Johnson, S. C., Rabinovitch, P. S. & Kaeberlein, M. mTOR is a key modulator of ageing and age-related disease. *Nature.* **493**, 338–345. https://doi.org/10.1038/nature11861 (2013).
28. Jia, H. J. et al. Artesunate ameliorates irinotecan-induced intestinal injury by suppressing cellular senescence and significantly enhances anti-tumor activity. *International immunopharmacology.* **119**, 110205. https://doi.org/10.1016/j.intimp.2023.110205 (2023).

29. Wu, Y., Wang, X., Wu, W. & Yang, J. Mendelian randomization analysis reveals an independent causal relationship between four gut microbes and acne vulgaris. *Frontiers in microbiology.* **15**, 1326339. https://doi.org/10.3389/fmicb.2024.1326339 (2024).
30. Abotorabi, Z., Khorashadizadeh, M., Arab, M., Hassanpour Fard, M. & Zarban, A. Jujube and green tea extracts protect human fibroblast cells against UVB-mediated photo damage and MMP-2 and MMP-9 production. *Avicenna journal of phytomedicine.* **10**, 287–296 (2020).
31. Zhao, X., Qi, Y., Yi, R. & Park, K. Y. Anti-ageing skin effects of Korean bamboo salt on SKH1 hairless mice. *The international journal of biochemistry & cell biology.* **103**, 1–13. https://doi.org/10.1016/j.biocel.2018.07.010 (2018).
32. Bosch, R. et al. Mechanisms of Photoaging and Cutaneous Photocarcinogenesis, and Photoprotective Strategies with Phytochemicals. *Antioxidants (Basel, Switzerland).* **4**, 248–268. https://doi.org/10.3390/antiox4020248 (2015).
33. Lin, T. Y. et al. Protective Effects of Sesamin against UVB-Induced Skin Inflammation and Photodamage In Vitro and In Vivo. *Biomolecules.* **9**, https://doi.org/10.3390/biom9090479 (2019).
34. Su, L. J. et al. Reactive Oxygen Species-Induced Lipid Peroxidation in Apoptosis, Autophagy, and Ferroptosis. *Oxidative medicine and cellular longevity.* **2019**, 5080843. https://doi.org/10.1155/2019/5080843 (2019).
35. Feingold, K. R. The outer frontier: the importance of lipid metabolism in the skin. *Journal of lipid research.* **50**(Suppl), S417-422. https://doi.org/10.1194/jlr.R800039-JLR200 (2009).
36. Feingold, K. R. Thematic review series: skin lipids. The role of epidermal lipids in cutaneous permeability barrier homeostasis. *Journal of lipid research.* **48**, 2531–2546. https://doi.org/10.1194/jlr.R700013-JLR200 (2007).

Acknowledgements

This work was financially supported by the National Natural Science Foundation of China (Grant No. 81860158) and the Special Basic Cooperative Research Programs of Yunnan Provincial Undergraduate Universities' Association (grant NO. 202301BA070001-046).

Author contributions

Man Li (First Author): Conceptualization, Methodology, Validation, Formal analysis, Investigation, Data Curation, Writing—Original Draft. Yuchen Ge: Formal analysis, Investigation, Writing—Review & Editing. Shirui Bai: Software, Formal analysis, Validation. Jing Xia: Formal analysis. Guangming Wang: Resources, Funding acquisition. Yaxuan Zhang: Formal analysis, Validation. Yuanyuan Zhang (Corresponding author): Resources, Writing—Review & Editing. Xiaobo Wang (Corresponding author): Resources, Project administration, Writing—Review & Editing, Funding acquisition. Min Zhou (Corresponding author): Conceptualization, Methodology, Project administration, Writing—Review & Editing, Funding acquisition.

Funding

National Natural Science Foundation of China (Grant No. 81860158).

Declarations

Competing interests

The authors declare no competing interests.

Additional information

Supplementary Information The online version contains supplementary material available at https://doi.org/10.1038/s41598-024-81573-x.

Correspondence and requests for materials should be addressed to Y.Z., X.W. or M.Z.